Response of Egyptian Observatories to the Intense Storm on April 23, 2023

Aalaa Samy, Tareq Fahmy Abdullatif, Marwa Shaheen

Geomagnetic laboratory, Geomagnetic and Geoelectric Department, National Research Institute of Astronomy and Geophysics (NRIAG), 11421 Helwan, Cairo, Egypt.

Abstract

A comprehensive study was conducted to assess the response of the Egyptian magnetic observatories (Misallat 'MLT' & Abu Simble 'ABS') to the intense storm that occurred on April 23, 2023. This storm is currently recognized as the second most intense storm within the Solar Cycle 25. The storm has caused significant fluctuations in the components of the Earth's magnetic field (X, Y, and Z). This study includes data from the Egyptian observatories (MLT & ABS), the GOES-16 satellite, and nearby observatories in Alergia and Greece (TAM and PEG). Unlike previous studies that have focused on the impacts of magnetic storms on regional magnetic field observations, this research provides a significant approach and additional value by examining the response of local Egyptian observatories to such important phenomena. The data collected from the Egyptian observatories was correlated with other data sets from TAM, PEG, and the GOES-16 satellite. The GOES-16 data showed a significant response due to the interaction of the satellite with the incoming solar wind stream in the plasma medium. Ground observatories also recorded simultaneous behavior in the observed components, with the highest level of disturbance on April 23rd. However, some long-period changes were still visible due to typical diurnal variation. To extract variations within the magnetic pulsations range, magnetic data was subjected to appropriate filtering techniques. High-pass filtering was applied by subtracting a time series moving average with a window of 100 samples from the measured time series. The study revealed storm-generated pulsations in the magnetosphere, with maximum pulse amplitudes of -101nT for Goes16, 13nT for MLT, and 7nT for ABS observatories. The power spectrogram showed pulsations that occurred in the recovery phase of the magnetic storm. The results of this study have significant implications for improving our understanding of space weather physics, forecasting, and mitigation procedures required.

Keywords: Magnetic storm; Misallat; Abu Simble; pulsations, Pc5; space weather.

1- Introduction:

Space weather is caused by the huge amount of energy naturally emitted by the Sun, which, in turn, reaches the Earth through the solar wind. This energy interacts impressively with the Earth's magnetic field and causes a disturbance that is known as a magnetic storm. Although humans may not feel these disruptions, they can have a serious impact on electrical infrastructure, interfere with radio communication, and even can affect GPS systems, and sometimes cause temporary outages of power stations **(Gaunt and Coetzee, 2007)** and disruption of satellite operation.

Furthermore, high-altitude pilots and astronauts may be exposed to excessive radiation levels during the occurrence of these events (i.e. magnetic storms). It is therefore very important to study these events to understand how the space weather phenomena behave and to develop all possible strategies for necessary mitigation measures. This is importantly needed for a safe and modern society. Geomagnetic observatories around the world can monitor such events in real time, providing invaluable information for understanding their behavior, effects, and implications.

The intense storms are caused by various phenomena such as solar coronal mass ejection (CME), solar flare, co-rotating interaction region (CIR), fast stream, and more. CME is the release of billions of energetic particles from the sun along with its magnetic field. It takes usually a few days to reach the Earth, but in some cases, the most intense storms have been observed within 18 hours. The ideal solar wind conditions for creating geomagnetic storms are sustained periods of high-speed solar wind, lasting several to many hours, and a southward-directed solar wind magnetic field (opposite to the direction of Earth's magnetic field) at the dayside of the magnetosphere occurring magnetic reconnection. This reconnection effectively transfers energy from the solar wind into Earth's magnetosphere **(Gonzalez et al., 1994).** The storm's intensity can be measured using various indices such as the Kp index or the disturbance storm time (Dst) index, which quantify the disturbance in Earth's magnetic field.

The study of geomagnetic storms has a long history dating back to the early 1800s when von Humboldt **(Humboldt and von, 1808)** first recorded observations of magnetic storms. Furthermore, he introduced the term "*magnetic storm*" (or "*magnetischen Stürme*"), among other scientific terminologies **(Korte and Mandea, 2019)**. Since then, many researchers have conducted studies on this topic, including those conducted since the turn of the millennium. For instance, **Vieira et al. (2001)** studied the development of geomagnetic storms, analyzing three types of magnetic clouds and finding that 20% of intense storms grow in their main phases in three or more steps. **Metallinou et al. (2004)** examined the relationship between energy dissipation during storms and substorms by analyzing 53 magnetic storms with peak SYM H values ranging from -50 to -350 nT utilizing SYM H and AL geomagnetic indices. The study discovered a strong correlation between storm and substorm energy dissipation (r = 0.928), indicating a high level of coupling between the two. **Lakhina et al. (2006)** studied the effects of intense magnetic storms on spacecraft operation, navigation, and telecommunication during the periods of October 29-31 and November 20-21, 2003. They also discussed the relationship between storms and substorms. **Ghamry et al. (2016)** conducted a study on four geomagnetic storms that occurred between February 18 and March 2, detecting Pi2 pulsation at various observatories including the Egyptian observatories, and analyzing Van Allen's mission during this period. **Arafa-Hamed et al. (2019)** used a 3-axis fluxgate magnetometer to monitor magnetic phenomena during a magnetic storm from March 26 to March 29, 2017, in Ulu-Slim, Malaysia. The study found that the onset of the storm was observed on March 28, and noted the absence of typical diurnal variation of total field intensity. In addition, pulsation enhancement was found to be common around noon and continuous on March 28th due to magnetotail activities during the local night, with the magnetospheric breathing captured twice. **Nahayo et al. (2019)** examined the response of southern African magnetic observatories to the Saint Patrick's Day storm and explored how this network of observatories could be utilized to model induced electric fields. The study uncovered discrepancies between global and local indices and demonstrated that these differences fluctuate in the storm's various phases. This information is crucial for monitoring anomalous currents caused by geomagnetic storms, which can potentially damage power distribution infrastructure.

It became clear that a key focus of space physics research was to investigate the processes by which the magnetosphere generates both storms and substorms in response to fluctuations in solar wind strength. This includes examining how the magnetosphere responds to energy absorption from the solar wind, leading to the emergence of two distinct phenomena

– geomagnetic storms and magnetospheric substorms **(Akasofu, 2021).** However, the study of geomagnetic storms is a significant challenge in space physics for several reasons. First, each magnetic storm has distinct features and general characteristics. Second, the occurrence of magnetic storms is influenced by various factors such as solar wind parameters, space weather conditions, geographic coordinates, local time, and the phase of the solar cycle **(Chernogor, 2024)**. Therefore, this study focuses on the response of the Egyptian observatories (MLT & ABS) to the intense magnetic storm that occurred on April 23, 2023, including the onset, peak intensity, duration, and associated solar wind conditions. This storm is currently considered the second most intense storm in the Solar cycle 25. In addition, a comparison of data from the Egyptian observatory, the nearest INTERMAGNET observatories, and the respective satellite will be conducted.

The research is organised as follows: Section 2 covers the data sources and sets. Section 3 discusses the solar wind conditions and how the Egyptian observatories and INTERMAGNET station responded to the intense storm. Section 4 describes the observed phenomena during the storm. In Section 5, the results are discussed. Finally, Section 6 provides a conclusion.

2- Data Sources:

The data sources utilized in this research include: 1. Egyptian observatory data, available from MLT and ABS observatories. 2. INTERMAGNET, the International Real-time Magnetic Observatory Network that provides observatory data worldwide. 3. The GFZ website, offers data for the Kp index **(Matzka et al., 2021)**. 4. The WDC Kyoto website, where Dst data can be accessed. 5. Magnetic satellite data from the GOES-R series, provided by the National Oceanic and Atmospheric Administration (NOAA). 6. Solar wind parameters obtained from NASA Space Physics Data Facility website **(Natalia and Joseph, 2020)**.

Data from two Egyptian geomagnetic observatories, the Misallat Observatory (MLT) and the Abu Simbel Observatory (ABS), were used for comparison with other data from nearby observatories belonging mainly to The INTERMAGNET network, the Tamanrasset Observatory (TAM) in Algeria and the Pedeli Observatory (PEG) in Greece. **Figure (1)** provides a location map of the four observatories associated with this study. **Table (1)** summarizes their basic information and related details.

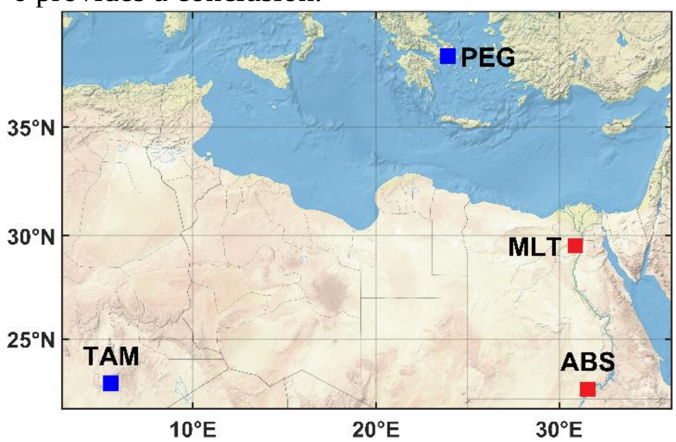

Figure 1: *The Egyptian observatories are highlighted in red, while the nearest INTERMAGNET stations are marked in dark blue.*

***Table 1**: The Egyptian geomagnetic observatories and the two INTERMAGNET stations*

IAGA Code	**Name**	**Country**	**Geographic Coordinates**		**Magnetic Coordinates**		**Institute(s)**
			Lat.	*Long.*	*Lat.*	*Long.*	
MLT	Misallat	Egypt	29.5N	30.9E	28.9 N	108.8 E	**National Research of Institute of Astronomy and Geophysics (NRIAG)*
ABS *not included*	Abu Simbel		22.5N	31.5E	19.5 N	107.7 E	
TAM	Tamanrasset	Algeria	22.8N	5.5E	24.4 N	82.2E	**Institut de Physique du Globe de Paris (IPGP) *Centre de Recherche en Astronomie, Astrophysique et Geophysique (CRAAG)*
PEG	Pedeli	Greece	38.1N	23.9E	36.4 N	103.6 E	**Institute of Geology and Mineral Exploration (IGME)*

3- Analysis and Results

3.1. Sun and solar wind activity:

On April 21st, 2023, the energetic Solar Active Region, known as NOAA AR 13283, located at S20W15, erupted a halo Coronal Mass Ejection (CME). This CME moved towards the Earth and generated an intense geomagnetic storm on April 23rd at 19:26 UT **(Ghag et al., 2024).** The storm was particularly severe and caught the attention of scientists and space weather forecasters worldwide. **Figure (2)** illustrates the generation mechanism of geomagnetic storms and auroral substorms when solar wind disturbances penetrate the magnetosphere. The diagram **(Fig. 2)** is modified after **Akasofu (2021)** and applied to the magnetic storm of April 23, 2023. The diagram includes 2a- a large coronal hole in the sun's southeast, 2b- an image of the sun captured at 304 angstroms, 2c- a cross-section of the magnetosphere showing solar wind and magnetic field lines, 2d- the AE index of the storm indicating depression in the Earth's magnetic field, and 2e- the appearance of aurora in high-latitude regions due to the storm.

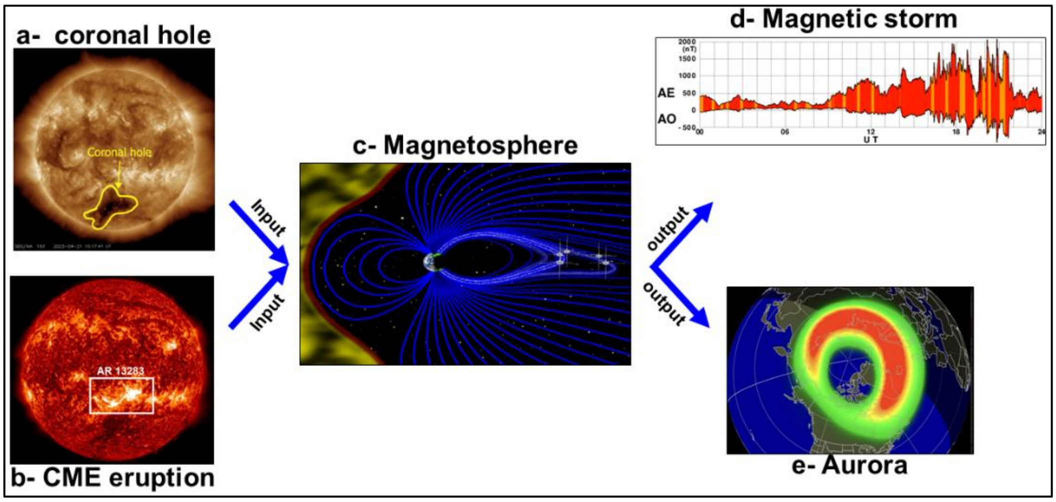

Figure 2: The mechanism of geomagnetic storms and auroral substorms generation when the magnetosphere receives solar wind disturbances as input. This diagram is modified after Akasofu (2021) and applied to the magnetic storm on April 23, 2023. a) a large coronal hole in the sun's southeast-NASA's Solar Dynamics Observatory (SDO). b) An image of the sun captured at 304 angstroms by the Atmospheric Imaging Assembly (AIA 304), which shows the location of AR 13283 as the source region of the CME eruption that took place on April 21, 2023, at 18:00 UT-SDO. c) A cross-section of the magnetosphere that displays the solar wind (in yellow) on the left and the magnetic field lines originating from the Earth (in blue) in response to the CME eruption-Emmanuel Masongsong/UCLA EPSS/NASA. d) The AE index of the concerned storm indicates the depression in the Earth's magnetic field - WDC. e) The appearance of aurora in high-latitude regions due to the storm-NOAA.

The interplanetary medium showed a moderate to high level of solar wind activity due to the interaction of CME with the Earth's magnetosphere. In **Figure (3)**, the evolution of the intense storm is depicted through the representation of seven solar wind parameters on a 1-minute basis. These parameters comprise the interplanetary total magnetic field (IMF B), the south component of the interplanetary magnetic field (IMF Bz), velocity (V), density (D), temperature (T), dynamic pressure (P), and electric field (Ey). During periods of low activity, the intensity of the IMF B and Bz components typically does not exceed ±5 nT. However, there was a significant increase in these components during the intense storm with IMF B_{max} ≈ 40 nT On April 24th, 2024 at 03:30, IMF B_{min} ≈ 5 nT, Bz_{max} ≈ 28 nT, and Bz_{min} ≈ – 36 nT on Apr 24th at 02:30 UT during the interaction of the CME with the inner magnetosphere. Likewise, the solar wind velocity was observed at a background level of 330-400 km/s before the storm. During the storm, the velocity increased by 751.7 km/s on April 23rd at 21:30 UT. Similarly, the proton density peaked at 30 n/cc on Apr 23rd at 19:30 from a background level of 1-23 n/cc due to the interaction with the interplanetary structure. The temperature also increased by 31x10^5 K from a background level of 1-2x10^5 K. These changes were accompanied by an increase in the dynamic pressure of 19.48 nPa from a background level of 1-3 nPa and an increase in the electric field of 10 mV/m from a background level of 1-4 mV/m.

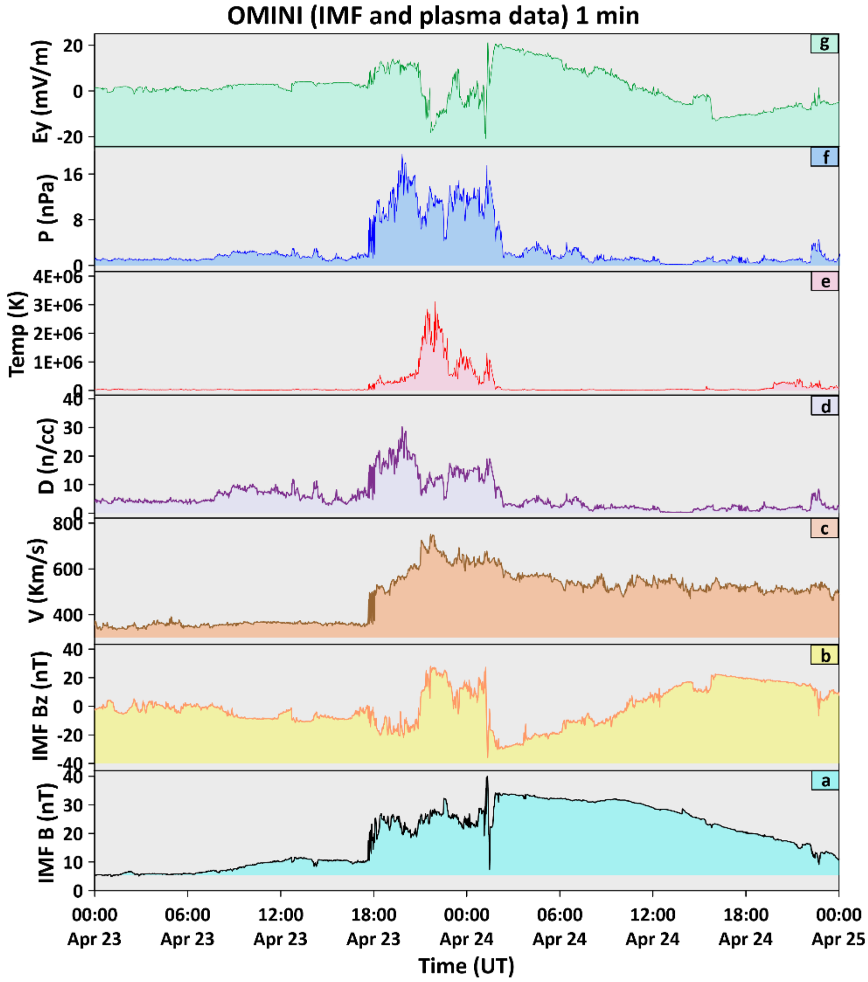

Figure 3: The changes in solar wind parameters due to the ICME interaction with the plasma in the interplanetary medium caused an intense storm on April 23-24, 2023. This interaction caused changes in various solar wind parameters showing the following variations: (a) the total interplanetary magnetic field (IMF B), (b) the variation in the south component of the IMF (IMF Bz), (c) the solar wind velocity, (d) the solar wind density, (e) the solar wind temperature, (f) the solar wind pressure, and (g) the solar wind electric field.

3.2. Geomagnetic Activity:

3.2.1. The Magnetic Indices:

The magnetic indices indicate the activity level in the Earth's magnetic field during certain periods. These indices are derived from magnetometer records in geomagnetic observatories, as explained by McPherron in 1995 **(McPherron, 2005)**. There are various types of indices, but only the kp and Dst indices will be discussed in this study. Briefly, the 3-hour K integer index was introduced by **Bartels in 1938**. It is used to measure the range of irregular and rapid storm-time magnetic activity. On the other hand, the Dst index developed by **Sugiura in 1964** is used to measure the intensity of the ring current.

On the afternoon of April 23, 2023, an intense storm occurred and caused a severe G4-level geomagnetic disturbance, lasting approximately 21 hours during the main phase. This was the first two-step severe geomagnetic storm in the Solar Cycle 25 caused by a coronal mass ejection that arrived the Earth at 19:26 UTC on April 23, 2023 **(Ghag et al., 2024)**.

The storm affected the geomagnetic indices, including the kp and Dst indices. The kp index is represented in the top panel of Figure (4) and indicates the level of magnetic disturbance. The color of the Kp index indicates the level of disturbance, with green being quiet (0-3), yellow being moderate (3-6), and red being active (6-9). The background Kp index varied in magnitude from 0 to 3, but it increased from 4 to 8.3 on the afternoon of April 23, 2023, before decreasing back to 3 on the afternoon of April 24, 2023. During the main phase of the storm, the Kp index values rose to a maximum of 8.33.

The Dst index, on the other hand, is represented in the bottom panel of **Figure (4)**. Before 09:00 UT on April 23, 2023, the magnitude of Dst varied from -14 nT to -8 nT. Between 09:00 UT and 21:00 UT on April 23, 2023, its magnitude decreased from -27 nT to -165 nT. There was a further decrease from -165 nT to -213 nT between 01:00 UT and 05:00 UT on April 24, 2023. After that, the strength of Dst increased from -213 nT to -56 nT at 23:00 UT on April 24, 2023, indicating a strong and long-lasting geomagnetic storm. The storm lasted for approximately 21 hours during the main phase, followed by a prolonged recovery phase on April 25, 2024.

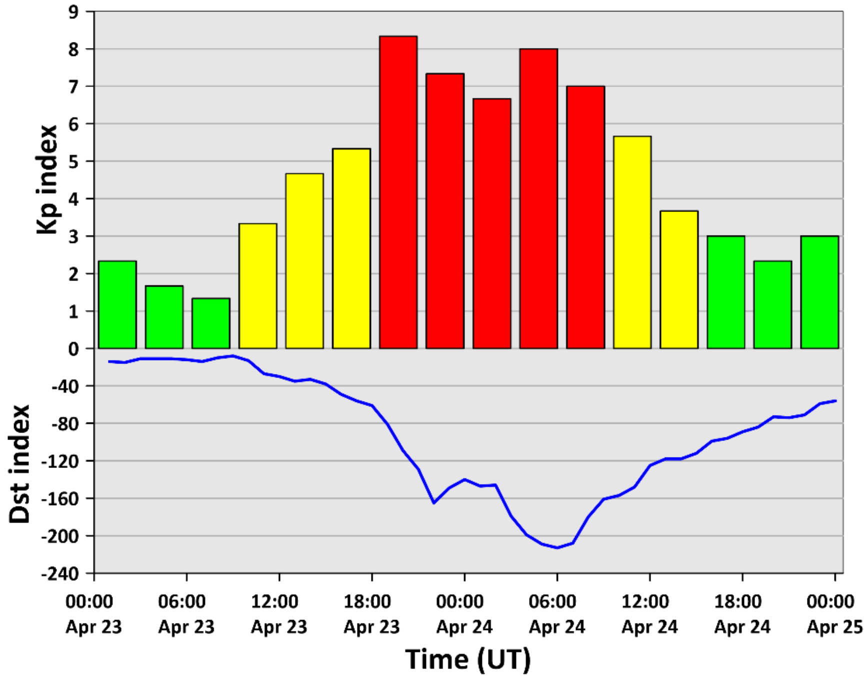

Figure 4: a) The Dst index started to decrease around 08:00 UT on April 23. It reached its value of -213 nT at 05:00 UT on April 24, indicating a strong and long-lasting geomagnetic storm. The main phase of the storm lasted for approximately 21 hours, followed by a prolonged recovery phase on the next day (April 25, 2024). b) The histogram displays the distribution of Kp index values, where red, yellow, and blue bars represent index values of 0-3 for quiet, 3-6 for moderate, and 6-9 for active, respectively. During the main phase of the storm, the Kp index values rose to a maximum of 8.33, indicating a severe G4-level geomagnetic storm according to space weather classification.

3.2.2. The Egyptian Geomagnetic Observatories Response:

The observatories in Egypt recently detected significant fluctuations in the three components (X, Y, and Z) of the Earth's magnetic field. To investigate this further, magnetic data from GOES-16 and the closest observatories TAM and PEG were used. **Figure (4)** indicates the time series from 00:00 UT April 23, 2023, to 00:00 UT April 25, 2023, and displays the response of the Egyptian geomagnetic observatories, GOES-16 satellite, and the TAM and PEG observatories to the intense storm that occurred on April 23, 2023. The upper, middle, and lower panels represent the variation of the Z, Y and X components, respectively. The y-axes have been removed to reveal the signature behavior in space and on the ground. The scale is shown in the lower panel.

According to data from the magnetic storm catalogue of Kakioka Magnetic Observatory, a sudden storm began at 17:35 UT on April 23, 2024, with the main phase occurring at 21:00 UT. The recovery phase lasted until 04:00 UT on April 25, 2024. The GOES-16 data revealed a significant response due to the satellite's presence in the plasma medium, which resulted from the interaction with the incoming solar wind stream. Additionally, the ground observatories also recorded simultaneous behavior in the observed X, Y and Z components, indicating the highest level of disturbance on April 23rd. Despite this, some long-period changes were still visible due to the typical diurnal variation. Thus, the period from noon on April 23rd to noon on April 24th marked the maximum effect of the magnetic storm that occurred following the injection of solar-wind particles into the magnetosphere.

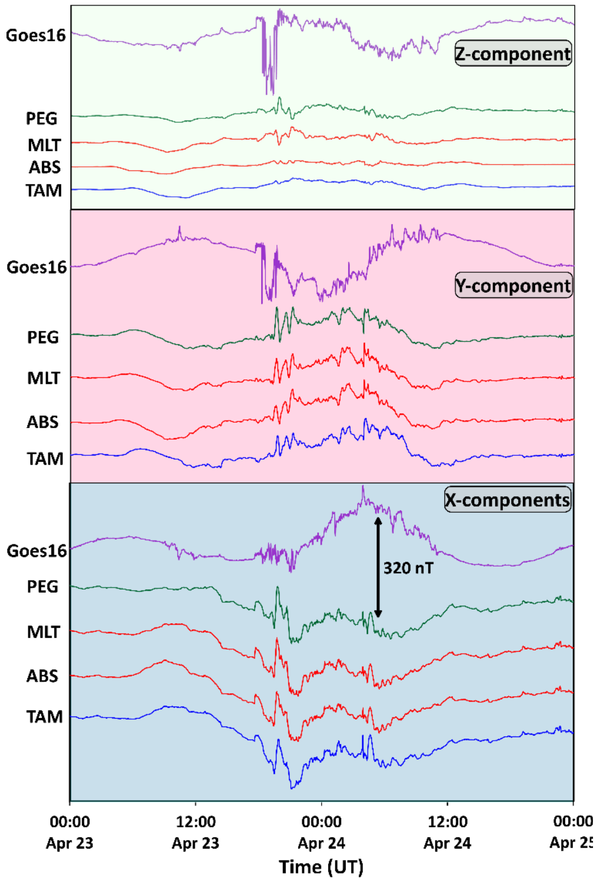

Figure 5: The response of the GOES-16 satellite, Egyptian geomagnetic observatories, PEG, and TAM observatories to the April 23, 2023 intense storm. The upper, middle and lower panels represent the variation of the Z, Y and X-components, respectively. All plots have a provided scale of 320nT.

3.2.3. Observed Phenomena: Geomagnetic Pulsations

In 1861, the first recorded observations of pulsations in the Earth's magnetic field were made by **Stewart, 1861**. These pulsations, known as ultra-low frequency (ULF) waves, have periods ranging from 0.2 to 600 seconds. In 1963, during the Berkeley Meeting, IAGA recommended two types of magnetic pulsations based on their forms: continuous (Pc) and irregular (Pi). Subsequently, sub-classifications were recognized based on the periods of the pulsations, which were designated as Pc1 to Pc5 and Pi1 to Pi2 **(McPherron, 1995 and Glassmeier et al., 2009)**. Picking up the magnetic pulsations associated with a geomagnetic storm is considered critical and important in this study. Pulsations provide additional storm parameters and play a vital role in space weather forecasting. These pulsations also aid in the diagnosis of Earth's magnetosphere by indicating substorm onsets and intensifications. Additionally, they assist in determining plasma density and tracking plasmapause temporal variations **(Saito et al., 1976)** and **(Menk et al., 2004)**.

Despite being pulsations classified as ULF Magneto Hydro Dynamic waves (MHD), geomagnetic pulsations have a higher frequency compared to the long-period diurnal variations that are usually observed at the observatory. As a result, it is essential to filter the recorded magnetic data to extract variations with periods within the acceptable magnetic pulsations' range. With a sampling rate of 1Hz, the Pc1 types cannot be considered due to the restricted Nyquist frequency **(Arafa-Hamed et al., 2019).** The high pass filtered data F(tp) is obtained by subtracting a moving average time series with a window of 100 samples from the measured time series (Ft).

$$\boldsymbol{F(tp) = Ft - \frac{\sum_{t-50}^{t+50} Ft}{100}} \quad \textbf{.........(1)}$$

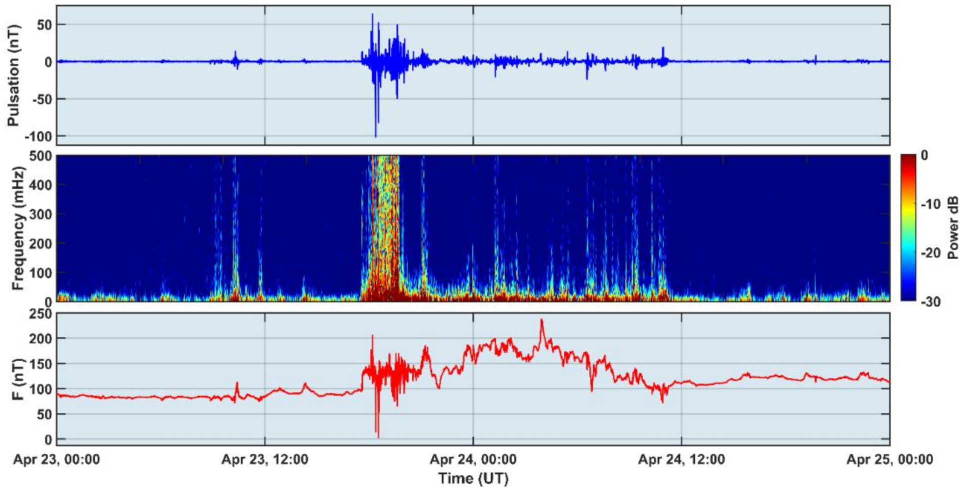

Figure 6: The total magnetic field (F) recorded by GOES-16 (lower panel). The middle panel displays the power spectrogram of the magnetic pulsations after applying a high-pass filter. The upper panel depicts the magnetic pulsations resulting from filtering out the long-period diurnal variation. The upper and middle panels demonstrate a clear increase in pulsation intensity after the onset of the storm. Despite the recovery of the typical diurnal variation on April 24^{th}, the intense occurrence of pulsations persisted as indicated by the three panels.

In **Figures (6, 7, and 8)**, the upper panels display high-frequency signals (Ftp) that reveal a distinct amplification of pulsations from the onset of the storm on April 23 at 17:35 UT to April 24 at midnight UT. This amplification is a clear indication of storm-generated pulsations in the magnetosphere, with maximum pulse amplitudes of -101nT at approximately 18:30 UT on April 23 for GOES-16, 13nT at around 04:00 UT on April 24 for MLT, and 7nT at about 04:00 UT on April 24 for ABS. In the middle panels of **Figures (6, 7, and 8)**, the power spectrogram calculated for the pulsation signal is displayed, reflecting the change in frequency content with time **(Schillinger and Papadopoulos, 2010)**. The spectrogram helps to interpret the continuous intensive pulsations observed from the storm onset until around 09:00 UT the next day. In the lower panel of **Figures (6, 7, and 8)**, the pulsation graph in correlation with the total field, F, provides a general overview of how pulsations are indicative of magnetic storms. Although the diurnal variation form of the total field is almost recovered, the sustained occurrence of intensive pulsations reveals the ongoing magnetic storm. It is worth noting that despite the noise present in both Egyptian observatories MLT and ABS **(Samy and Arafa-Hamed, 2023)**, the pulsations are still clearly observed.

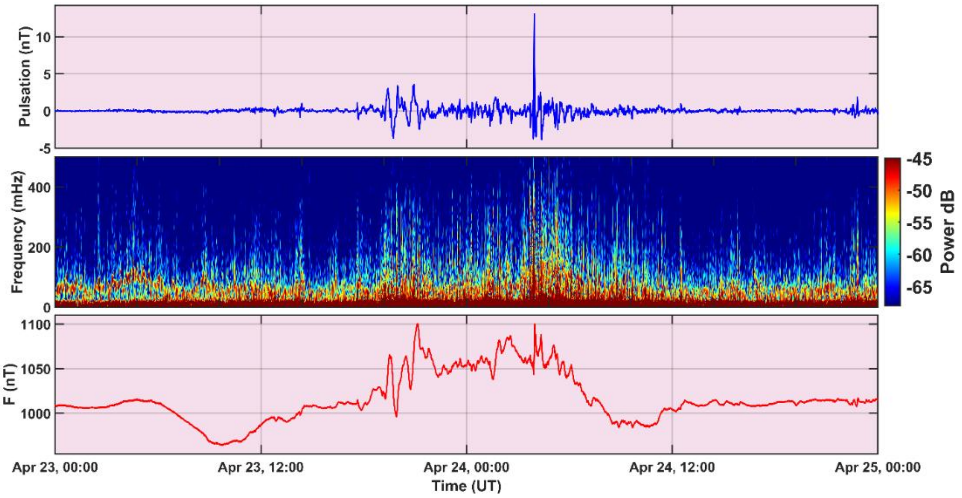

Figure 7: The total magnetic field (F) recorded by MLT (lower panel). The middle panel displays the power spectrogram of the magnetic pulsations after applying a high-pass filter. The upper panel depicts the magnetic pulsations resulting from filtering out the long-period diurnal variation. The upper and middle panels demonstrate a clear increase in pulsation intensity after the onset of the storm. Despite the recovery of the typical diurnal variation on April 24th, the intense occurrence of pulsations persisted as indicated by the three panels.

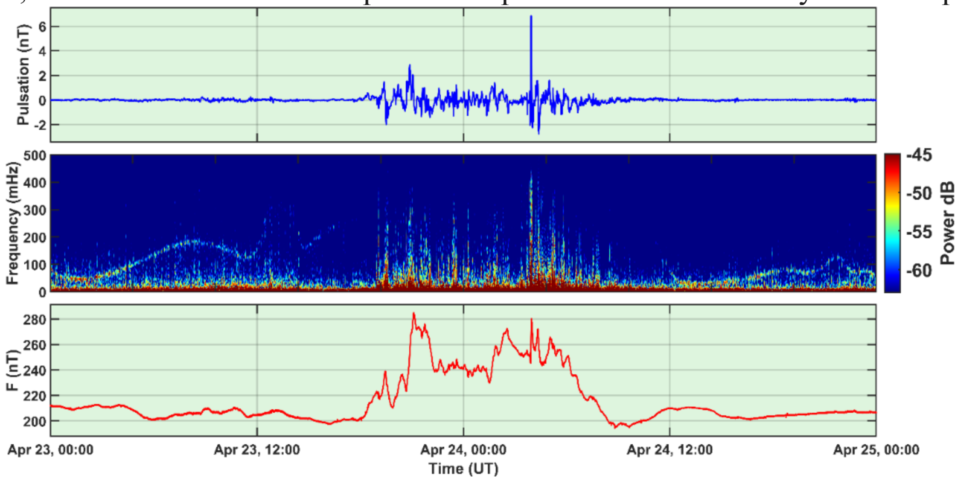

Figure 8: The total magnetic field (F) recorded by ABS (lower panel). The middle panel displays the power spectrogram of the magnetic pulsations after applying a high-pass filter. The upper panel depicts the magnetic pulsations resulting from filtering out the long-period diurnal variation. The upper and middle panels demonstrate a clear increase in pulsation intensity after the onset of the storm. Despite the recovery of the typical diurnal variation on April 24th , the intense occurrence of pulsations persisted as indicated by the three panels.

We utilized the magnetic data of GOES16, MLT, and ABS to conduct a thorough analysis to investigate the Pc5 pulsation. This type of pulsation typically lasts a few minutes, with a period ranging from 150 to 600 seconds. Its rotation direction is usually counterclockwise in the morning and clockwise in the evening, as noted by **Sano in 1963**. Due to its significant amplitudes and long periods, it is the most easily detectable ULF wave. Even magnetograms with low sensitivity and sampling rates as low as 1 minute can detect it. In addition, the Pc5 pulsation plays a critical role in the acceleration of electrons to relativistic energies in the outer radiation belt through the process of drift resonance, as demonstrated by **Elkington et al. (1999)** and **Degeling et al. (2007)**.

To capture Pc5 pulsations, a band-pass filter with a passband frequency ranging from 1.67 mHz to 6.7 mHz was utilized. In **Figure (9)**, the total magnetic field (F) is illustrated in blue, while the corresponding ULF Pc5 pulsation band is highlighted in red. **Figure (9a, b and c)** represents the GOES-16 satellite data, the MLT and ABS ground observatory data. During storm time, the Pc5 is observed to be enhanced in both satellite and ground data, as evidenced by the general similarity of the signals in the MLT and ABS observatories. The band-pass filter indicates that the main peak appears at around 18:30 UT on April 23 for the GOES-16 satellite and 04:30 UT on April 24 for the MLT and ABS ground stations. It is noteworthy that the Pc5 maximum amplitude exceeds 15 nT for GOES-16, 10 nT for MLT, and 5 nT for ABS.

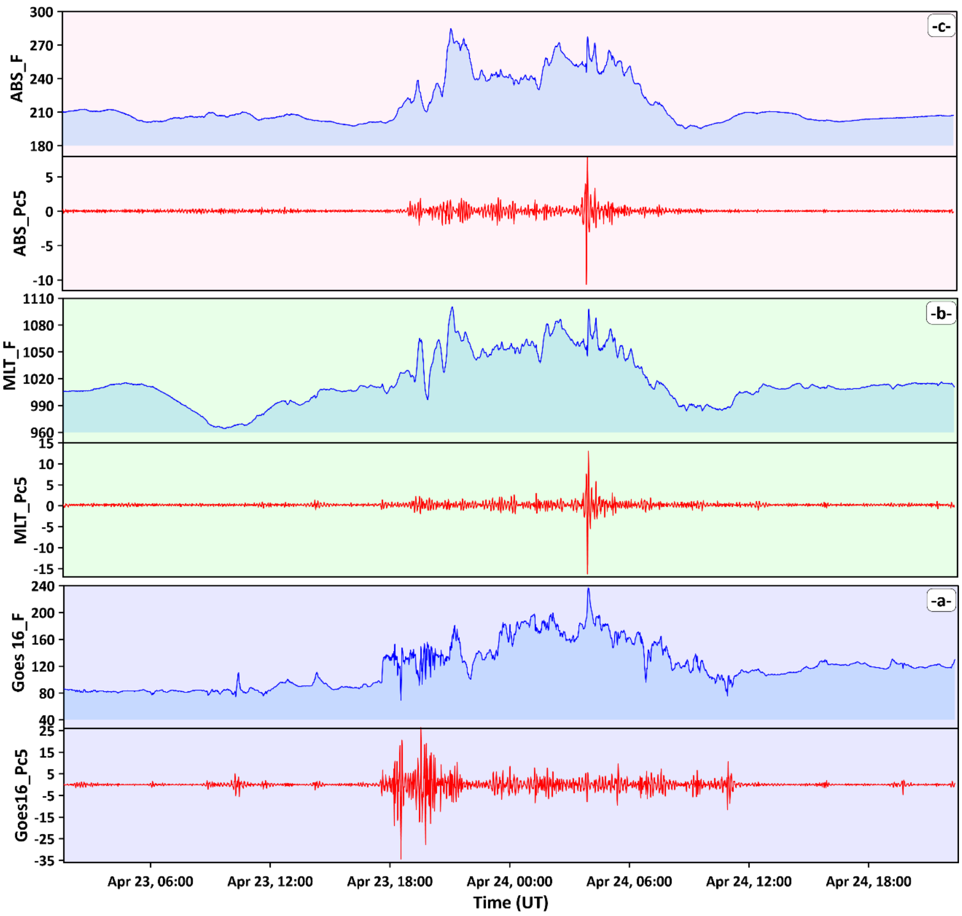

Figure 9: The total magnetic field F (raw data) in blue and the corresponding ULF Pc5 pulsation (bandpass filtred) in red. a) GOES-16 satellite, b) MLT observatory, c) ABS observatory.

4- Discussion

The geomagnetic storm that occurred on April 23, 2023, was one of the most intense events observed during the solar cycle 25 associated with ICME **(Habarulema et. al., 2024)**. Discussing the analyzed data collected from satellites and ground-based observatories is an important step that contributes to improving our understanding of the response of Egyptian observatories (MLT & ABS) to the effect of this storm, in particular, studying the behavior of the component of the Earth's magnetic field during the storm.

The storm was characterized by a significant increase in the Kp index up to 8.33 and a sharp decrease in the Dst index down to -213 nT. This indicates a severe disturbance in the Earth's magnetosphere, with the storm lasting for 21 hours followed by a prolonged recovery phase. The observed fluctuations in the X, Y, and Z components of the magnetic field at the Egyptian observatories are consistent with the global-scale effects of this intense geomagnetic storm.

Remarkably, the response recorded by the GOES-16 satellite showed a more pronounced signature compared to the ground-based observatories. This is likely due to the satellite's direct interaction with the incoming solar wind stream in the plasma medium, which can induce stronger magnetic perturbations. While, the ground-based observatories, still record significant disturbances. The results of the applied high-pass filter revealed that the storm generated pulsations with maximum amplitudes of -101 nT for GOES-16, 13 nT for MLT, and 7 nT for ABS. The power spectrogram analysis further confirmed the presence of pulsations indicative of magnetic storm activity, including enhanced Pc5 pulsations.

The enhanced Pc5 pulsations observed in both satellite and ground-based data during the storm period are particularly noteworthy. These pulsations are detected during the recovery phase of the storm as proven by **Setsko et al. (2023)**. These long-period pulsations can have significant implications for the operation of power networks and other technology-based systems, as they can induce geomagnetically induced currents (GICs) that can disrupt infrastructure **(Despirak et al., 2024)**. The maximum amplitude of Pc5 observed in this study exceeded 15 nT for GOES-16, 10 nT for MLT, and 5 nT for ABS, emphasizing the possibility of severe effects of space weather in the Egyptian territory. The findings of this study have important implications for our understanding of space weather phenomena and their effects on technological systems, particularly in the Egyptian context. The comprehensive dataset, incorporating both satellite and ground-based observations, provides valuable observations that can contribute to improving space weather forecasting and developing mitigation strategies to protect critical infrastructure.

Furthermore, the data from the Egyptian observatories used in this analysis can play a vital role in advancing our knowledge of the spatial and temporal dynamics of geomagnetic storms. The unique geographic location of these observatories, situated at relatively low latitudes, offers an opportunity to study how magnetic disturbances propagate and manifest in this region, which is often underrepresented in the wider landscape of space weather research.

5- Conclusion:

Studying the response of Egyptian observatories (MLT & ABS) to the intense storm on April 23, 2023, is extremely important to assess their performance during such an important space event that often does not regularly occur with this noticeable intensity.

The occurrence of this storm, which is recognized as the second most intense storm within the Solar cycle 25, enabled researcher all over the world to carry out several studies and analysis to develop and update their knowledge and catalogues in the field of magnetic observations whether on the ground or in the space.

This study analyzed and investigated the response of the Egyptian observatories in Fayoum (MLT) and Abu Simbel (ABS) to the intense geomagnetic storm of April 23, 2023. The storm is characterized by high Kp (8.33) and low Dst (-213 nT) indices, lasting 21 hours with a prolonged recovery phase. The analysis of magnetic data includes data sets from GOES-16 satellite, and ground-based observatories of Egypt (MLT & ABS), Algeria (TAM), and Greece (PEG).

According to the statistical analysis applied to all data sets collected from different sources, this study concluded the importance of continuous monitoring and analysis of geomagnetic data, especially from observatories in understudied countries like Egypt. The results can be summarized as follows:

- Egypt's geomagnetic observatories indicated significant fluctuations in the components (X, Y, and Z) of the Earth's magnetic field on April 23, 2023.
- The GOES-16 data showed a significant response due to the satellite's interaction with the incoming solar wind stream.
- Ground observatories (MLT, ABS, TAM, and PEG) also recorded simultaneous behavior in the observed components, with the highest level of disturbance on April 23^{rd}.
- The application of high-pass filtering was truly useful and important to extract variations within the magnetic pulsations' range, revealing storm-generated pulsations with maximum amplitudes of -101 nT for GOES16, 13 nT for Misallat (MLT), and 7 nT for Abu Simbel (ABS).
- Power spectrogram analysis confirmed the presence of pulsations indicative of magnetic storm activity, including enhanced Pc5 pulsations during the storm.
- The findings have significant implications for the importance of Egyptian observatory data in improving the understanding of space weather physics, forecasting, and mitigating its effects.

Conflict of interest statement

The corresponding author states that there is no conflict of interest.

Data availability statement

The data from the Egyptian observatory that supports the findings of this study can be requested from the corresponding author. The data from TAM and PEG observatories are available on the INTERMAGNET website (https://imag-data.bgs.ac.uk/GIN_V1/GINForms2), while Kp index data can be obtained from The GFZ website (https://kp.gfz-potsdam.de/en/data). The Dst index data are available on the WDC Kyoto website (https://wdc.kugi.kyoto-u.ac.jp/dst_realtime/index.html). Additionally, magnetic satellite data from the GOES-R series can be accessed on the NOAA website (https://www.ngdc.noaa.gov/stp/satellite/goes-r.html), and solar wind parameters can be obtained through the NASA Space Physics Data Facility (https://cdaweb.gsfc.nasa.gov/index.html).

Funding

The author did not receive any funds, grants, or other support during the preparation of this manuscript.

Acknowledgements:
We would like to express our gratitude to the following stations and organizations for their cooperation and efforts in operating these stations and providing us with data for the real-time AE index: AE stations including Abisko (SGU, Sweden), Dixon Island, Cape Chelyuskin, Tixie Bay, Pebek (AARI, Russia), Barrow, College (USGS, USA), Yellowknife, Fort Churchill, Sanikiluaq (Poste-de-la-Baleine) (GSC, Canada), Narsarsuaq (DTU Space, Denmark), and Leirvogur (U. Iceland, Iceland); the RapidMAG team (NiCT, JHU/APL, UoA, AARI, IDG); British Geological Survey – Geomagnetism for providing model calculations for determining geomagnetic coordinates; National Research Institute of Astronomy and Geophysics for Egyptian observatory data; INTERMAGNET for providing observatory data worldwide; GFZ for offering data sources for the Kp index; WDC Kyoto website for Dst data availability; the National Oceanic and Atmospheric Administration (NOAA) for providing magnetic satellite data from the GOES-R series; and the NASA Space Physics Data Facility website for providing solar wind parameters.

References

Akasofu S-I (2021). A Review of Studies of Geomagnetic Storms and Auroral/ Magnetospheric Substorms Based on the Electric Current Approach. Front. Astron. Space Sci. 7:604750. doi: 10.3389/fspas.2020.604750.

Arafa-Hamed, T., Khalil A., Nawawi M., Hassan, H., Arifin, M.H. (2019) *Geomagnetic phenomena observed by a temporal station at Ulu-Slim, Malaysia during the storm of March 27, 2017.* Sains Malaysiana, 48 (11). pp. 2427-2435. ISSN 0126-6039, http://dx.doi.org/10.17576/jsm-2019-4811-13.

Chernogor, L. (2024), Characteristic features of latitudinal manifestations of the 23–24 April 2023 geomagnetic storm, Ann. Geophys. Discuss. [preprint], https://doi.org/10.5194/angeo-2024-9, in review.

Degeling, A.W., Rankin, R., Kabin, K., Marchand, R., Mann, I.R., (2007). The effect of ULF compressional modes and field line resonances on relativistic electron dynamics. Planet Space Sci., 55.

Despirak, I. , Setsko,P., Lubchich,A. Hajra, R. Sakharov, Y., Lakhina, G., Selivanov, V., Tsurutani, T., (2024), Geomagnetically induced currents (GICs) during strong geomagnetic activity (storms, substorms, and magnetic pulsations) on 23–24 April 2023, Journal of Atmospheric and Solar-Terrestrial Physics, 261, p. 106293. doi:10.1016/j.jastp.2024.106293.

Elkington, S.R., Hudson, M.K., Chan, A.A., (1999). Acceleration of relativistic electron via drift-resonant interaction with toroidal mode Pc5 ULF oscillations. Geophys. Res. Lett.

Gaunt CT, Coetzee G. (2007) Transformer failures in regions incorrectly considered to have low GIC-risk. IEEE PowerTech, Lausanne.:807–812. https://doi. org/10.1109/PCT.2007.4538419.

Ghag, K., Raghav, A., Bhaskar, A., Soni, S., Sathe, B., Shaikh, Z., Dhamane, O., Tari, P., (2024), Quasi-planar ICME sheath: A cause of the first two-step extreme geomagnetic storm of the 25th solar cycle observed on 23 April 2023, Advances in Space Research, ISSN 0273-1177, https://doi.org/10.1016/j.asr.2024.03.011.

Ghamry, E., Lethy, A., Arafa-Hamed, T., Abd Elaal, E , (2016) A comprehensive analysis of the geomagnetic storms occurred during 18 February and 2 March 2014, NRIAG Journal of Astronomy and Geophysics, 5:1, 263-268, https://doi.org/10.1016/j.nrjag.2016.03.001.

Glassmeier, K.H., Soffel, H. & Negendank, J.W. (2009). Geomagnetic Variations, Space-Time Structure, Processes, and Effects on System Earth. Heidelberg: Springer Verlag.

Gonzalez, W.D., Joselyn, J.A., Kamide, Y., Kroehl, H.W., Rostoker, G., Tsurutani, B.T., Vasyliunas, V.M., (1994). What is a magnetic storm? Journal of Geophysical Research 99 (A4), 5771–5792.

Habarulema, J. B., Zhang, Y., Matamba, T., Buresova, D., Lu, G., Katamzi-Joseph, Z., et al. (2024). Absence of high frequency echoes from ionosondes during the 23–25 April 2023 geomagnetic storm; what happened? Journal of Geophysical Research: Space Physics, 129, e2023JA032277. https://doi.org/10.1029/2023JA032277.

Humboldt, A. von, (1808). Die vollstandigeste aller bisherigen Beobachtungen ¨ uber ¨ den Einfluss des Nordlichtes auf die Magnetnadel. Gilb. Ann., 29.

Korte, M., & Mandea, M. (2019). Geomagnetism: From Alexander von Humboldt to current challenges. Geochemistry, Geophysics, Geosystems, 20, 3801–3820. https://doi.org/10. 1029/2019GC008324.

Lakhina, G.S., Alex, S., Mukherjee, S., Vichar, G. (2006) On magnetic storms and substorms. In: Gopalswamy, N., Bhattacharyya, A. (eds.) Proceedings of the ILWS Workshop, p. 320.

Matzka, J., Stolle, C., Yamazaki, Y., Bronkalla, O., Morschhauser, A., (2021). The geomagnetic Kp index and derived indices of geomagnetic activity. ISSN: 15427390 Space Weather 19, 1221. https://doi.org/10.1029/2020SW002641. e2020SW002641.

McPherron, R.L. (2005). Magnetic pulsations: Their sources and relation to solar wind and geomagnetic activity. Survey of Geophysics 26: 545-592.

McPherron, R.L., (1995). Standard indices of geomagnetic activity. In Kivelson, M.G., Russell, C.T. Introduction to Space Physics. Cambridge, UK: Cambridge University Press, pp. 451–458.

Menk, F.W., Mann, I.R., Smith, A.J., Waters, C.L., Clilverd, M.A., & Milling, D.K. (2004) Monitoring the plasmapause using geomagnetic field line resonances, J. Geophys. Res., 109, A04216, doi:10.1029/2003JA010097.

Metallinou, F. A., Daglis, I. A., Kamide, Y., Seiradakis, J.H., (2004), Study of the Dst-AL correlation during geospace magnetic storms, in *IEEE Transactions on Plasma Science*, vol. 32, no. 4, pp. 1455-1458, https://doi.org/10.1109/TPS.2004.831734.

Nahayo, E., Kotzé, P. B., Cilliers, P. J., & Lotz, S. (2019). Observations from SANSA's geomagnetic network during the Saint Patrick's Day storm of 17–18 March 2015. South African Journal of Science, 115(1/2). https://doi.org/10.17159/sajs.2019/5204.

Natalia E.P; Joseph H.K, (2020). OMNI 1-min Data Set [Data set]. NASA Space Physics Data Facility. https://doi.org/10.48322/45bb-8792 (CiteAs link). Accessed on 2024-April-02.

Saito, T., Yumoto, K., & Koyama, Y. (1976) Magnetic pulsation Pi2 as a sensitive indicator of magnetospheric substorm, Planet. Space Sci., 24, 1025-1029.

Samy, A., & Arafa-Hamed, T. (2023). Raw data denoising and assessment of records from Misallat and Abu Simbel geomagnetic observatories, Egypt. Journal of African Earth Sciences, 202(November 2022), 104941. Doi: 10.1016/j.jafrearsci.2023.104941.

Sano, Y., (1963). Morphological studies on sudden commencements of magnetic storms using rapid-run magnetograms (including studies on sudden impulses). Mem. Kakioka Mag. Obs., 11.

Schillinger, D. & Papadopoulos, V. (2010). Accurate estimation of evolutionary power spectra for strongly narrow-band random fields. Computer Methods in Applied Mechanics and Engineering 199: 947-960.

Setsko, P.V., Despirak, I.V., Sakharov, YaA., Lubchich, A.A., Bilin, V.A., Selivanov, V.N., 2023. Geoinduced currents on Karelian-Kola power line and Finnish gas pipeline on September, 12–13 2017. J. Atmos. Sol. Terr. Phys. 247, 106079 https://doi.org/10.1016/j.jastp.2023. 106079.

Stewart, B., (1861). On the great magnetic disturbance which extended from August 28 to September 7, 1859, as recorded by photography at the Kew Observatory. Phil. Trans. R. Soc. Lond. 423.

Sugiura, M., (1964). Hourly values of equatorial D st for the IGY. Annals of the International Geophysical Year, 35: 945–948.

Vieira, L., Gonzalez, W., Clua de Gonzalez, A., Lago, A., (2001), A study of magnetic storms development in two or more steps and its association with the polarity of magnetic clouds, Journal of Atmospheric and Solar-Terrestrial Physics, Vol. 63(5), Pages 457-461, https://doi.org/10.1016/S1364-6826(00)00165-6.